Hindawi
Journal of Nanomaterials
Volume 2022, Article ID 9916742, 11 pages
https://doi.org/10.1155/2022/9916742

Research Article

Effect of Alloying Elements and Ceramic Coating on the Surface Temperature of an Aluminum Piston in a Diesel Engine

S. Vengatesan[1,2] **Paras Yadav**[1] **and Edwin Geo Varuvel**[3]

[1]*Department of Automobile Engineering, College of Engineering & Technology, SRM Institute of Science and Technology, Potheri, Chengalpattu, 603203 Tamil Nadu, India*
[2]*Renault Nissan Technology & Business Centre India, Tamil Nadu, India*
[3]*Department of Mechanical Engineering, Faculty of Engineering and Natural Sciences, Istinye University, Istanbul, Turkey*

Correspondence should be addressed to Edwin Geo Varuvel; vedwingeo@gmail.com

Received 23 August 2022; Accepted 27 September 2022; Published 17 October 2022

Academic Editor: Jianbo Yin

The engine piston is subjected to very high temperature during the combustion process, and it is very difficult to control the stability of the geometry at elevated temperature. The stability of the engine piston was analysed by finite element method with steady-state conditions for three different types of approach to control it, where the influence of the alloying element of aluminum piston, influence of surface coating, and its impact on the thickness variation followed by the influence of holes on the coating surface have been analysed in detail. It is observed that the coating with holes shows good agreement with requirement compared to the influence of the alloying element and coated piston. The conduction mode of heat transfer is controlled, and also, the heat transfer to the adjacent components is facilitated by holes on the coated piston.

1. Introduction

The reduction in the temperature of the piston exterior, especially the throat temperature of piston, can be helpful in increasing the longevity of the piston, hence improving diesel engine overall reliability. Reduced piston surface temperature also prevents microwelding on the piston's second ring groove surface and lowers the production of surface carbon. Various alloying elements like Mg, Mn, Cu, Ni, Si, Zn, and Ti with different compositions are added to the aluminum alloy piston material which will help in reducing the piston surface temperature. Also, when ceramics are compared to metals on the basis of thermal properties, ceramics were found to be more durable than metals, so the cooling is not required as quickly as metals [1]. Ceramics also outperforms standard materials in terms of wear performance as found in the literature [2]. The temperature control of the piston and heat flow over the surface can be controlled by disadvantage of the ceramic material—poor thermal conductivity [3, 4]. Thermal barrier coatings have the ability to improve an engine's thermal efficiency and also to enhance combustion and reduce emissions. Many tests have been conducted to explore how these ceramic properties may be applied to increase thermal efficiency by decreasing the dissipation of heat and to increase efficiency of the mechanical system by removing the need for cooling systems. The heat is transferred to the exhaust since the loss in cylinder cooling rate is decreases. Thermal efficiency of engines with low heat desertion is improved by this strong energy recovery through exhaust [5]. Heat recovery structures, on the other hand, necessitate a significant amount of effort to install because they necessarily require multiple engine architecture changes. Even in the absence of heat recuperation equipment, part of the heat is used to power the pistons which

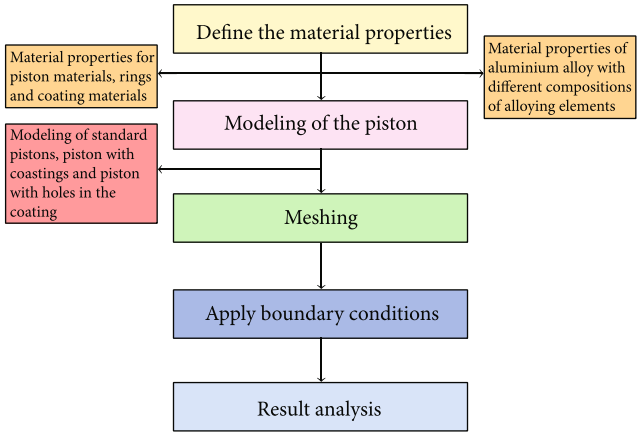

Figure 1: Basic methodology.

results with the increased thermal performance. Therefore, low heat desertion engines without exhaust heat recuperation equipment are worthy of being investigated. There is a layer known as bond coat layer in between the thermal barrier coating and the metal substrate. The adhesion of the thermal barrier coating and also the oxidation controlled by intermetallic alloy are called bond coating. The coefficient of expansion of the bond material lies between metallic and ceramic coating which is also suppressing the thermal shocking caused by the internal stresses [6, 7].

The stress distribution, combustion temperature, and temperature gradient are all influenced by the thickness of the coating. The thermal expansion coefficient, elastic modulus, and thermal conductivity of a ceramic coating define its thermal shock resistance [8, 9]. As a result, selecting the right thickness of the thermal barrier coating is critical not only for accurate temperature drop evaluation but also for the coated system's overall performance. This contribution will assist piston manufacturers in selecting parameters for the thermal efficiency of the piston material which will help in controlling the surface temperature of pistons and resulting in the improved efficiency of the piston at high temperatures.

Liu and his colleagues did a study of Cu and Ni and its impacts on the thermal characteristics of three types of aluminum-silicon (Al–Si) alloy piston materials. The crucial parameters such as specific heat capacity, thermal diffusion coefficient, and thermal conductivity are evaluated. Three types of engine aluminum alloy pistons were made under the identical circumstances. The piston surface temperature was determined using the hardness plug temperature calibration technique. Ansys commercial package is used for finite element analysis to model piston surface temperature field and analyse important piston components with temperature distribution. The finite element modelling findings of piston surface temperature field are compatible with hardness plug test temperature measurement data, and the temperature change of critical piston sites follows a similar pattern. Aluminum piston thermal conductivity rises with temperature. The piston head and skirt have different temperatures. High thermal conductivity lowers piston head temperature. Cu and Ni diminish thermal conductivity of aluminum alloys and raise piston surface temperature. Properly manipulating alloying components can influence piston heat resistance and high temperature performance [10].

Gehlot and Tripathi in their research analyse the steady-state thermal behaviour of ceramic-coated diesel pistons with holes. Ansys finite element software investigates piston top and substrate temperature distribution. Al–Si piston crown is coated with Yttria-stabilized zirconia as it is in the literature. Ceramic top coating thickness is 0.4 mm, while NiCrAl bond coat is 0.1 mm. Temperature distribution is studied using 1.5 mm, 2 mm, and 2.5 mm pores in ceramic coatings. The top surface (coated surface) temperature increases with increase in hole radius. As expected the Maximum surface temperature for 2.5 mm hole radius. Holed coatings raise piston surface temperature significantly compared to nonholed coatings, and also, increasing hole radius decreases substrate temperature [11].

In the light of the above discussion, the comparative study of pure metal piston, alloy piston, and coated piston was not addressed by any of the researchers to the author's knowledge. In this work, the comparative study of the abovementioned types is addressed using steady-state heat transfer analysis and compared in terms of surface temperature distribution over the piston.

The following contents are arranged as in the following: in Section 2, the detailed description of the model, boundary condition, coating material, and basic formulations in the finite element method are discussed. In Section 3, the influence of alloying elements, coated piston, influence of thickness of coating, and modified coating techniques are discussed elaborately. The variation in the temperature distribution is compared and concluded in the last section.

2. Methodology

The methodologies used in the analysis are as follows (Figure 1):

(i) To begin the simulation, Ansys commercial package is chosen and enabled the steady-state thermal analysis

(ii) Following that, the engineering data section defines the material properties of aluminum pistons with various alloying element compositions, as well as the structural and thermal properties of piston, rings, and coating materials are defined

(iii) After defining the material properties, a 3D modelling of the piston is modeled using SolidWorks software and saved as a .stl file. The geometry is imported to the geometry section of the selected module

(iv) The materials are assigned to specific components such as pistons, coatings, and rings under the model section. The piston's meshed model is then generated with optimal element size as per the recommendations. Then, the boundary conditions such as film coefficient and ambient temperature are

Table 1: Three AlSi alloy pistons with different compositions of elements [10].

Elements	Silicon	Copper	Magnesium	Nickel	Manganese	Titanium	Iron	Zinc
A1	12.15%	0.98%	0.97%	0.97%	0.08%	0.091%	0.30%	0.002%
A2	11.95%	3.47%	1.08%	1.87%	0.20%	0.093%	0.33%	0.005%
A3	12.33%	3.71%	0.94%	2.35%	0.31%	0.102%	0.43%	0.076%

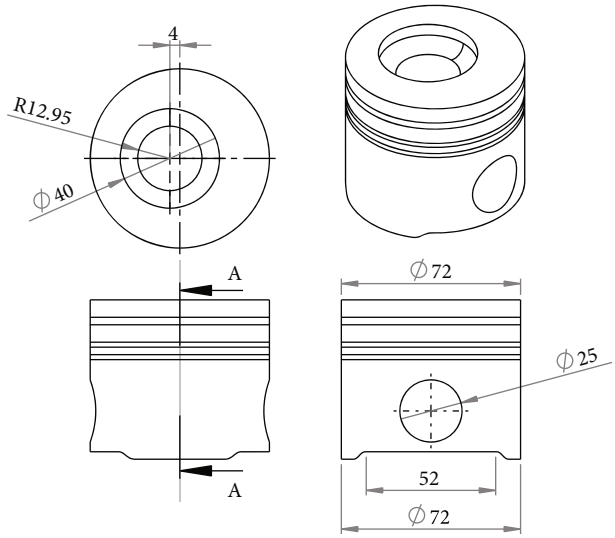

Figure 2: Geometry of the engine piston with standard layout with first angle projection.

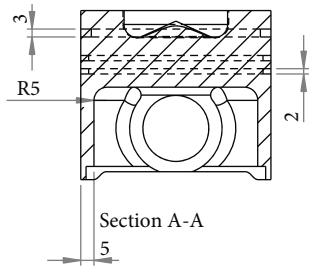

Figure 3: Cut sectional view of the geometry.

defined to various piston locations based on the literature [10]

(v) Postprocessing: the field variable temperature and its rate in change are plotted after solving the simulation

The variation in the alloying element, coating on the surface, and coating with holes is incorporated to the simulation accordingly in the preprocessing stage. The basic changes in the simulation are explained as follows for three conditions.

2.1. Aluminum Piston with Various Alloying Elements. The alloying elements are varied with base metal and compared the behaviour with conventional aluminum piston. The variation on the alloying elements are listed in Table 1. To run the simulation, the modelling part is the primary requirement in the simulation.

2.1.1. Establishment of Piston Model. The 3D solid model of the piston is modelled using SolidWorks modelling tool, and the dimensions of the model are taken from existing literature [12]. Half piston model is used as the analysis model in order to simplify the solving stage since it is symmetric about the axis and also utilize the maximum efficiency of calculation. The model is then split into a single grid size division, which is subsequently divided further to follow the thumb rule. The component with thin sections and surface with less temperature gradient have higher gradient compactness, whereas grid compactness is reduced in regions with bigger characteristic surface and a minor temperature gradient, which helps to better the computation precision and efficiency. Engine piston geometry with standard layout and first angle projection is illustrated in Figure 2, and cut sectional view of geometry is demonstrated in Figure 3. The piston assembly's 3D solid model and meshed model are shown in Figure 4.

Conduction, convection, and radiation are the three basic ways of heat transfer modes with variation in temperature. Because of the intricacy of heat exchange between elements as an engine burns in cylinder, it is very difficult to identify the temperature, making it impossible to determine precise thermal boundary conditions. The most popular approaches for transferring gas heat are radiation and convection. Radiant heat transfer accounts for a very modest percentage of total heat transfer. Observing and studying the literature help to determine the most of the boundary parameters of each piston surface [10, 13]. In order to analyse heat transfer in the piston, the fundamental methodology steady-state convection is followed in the entire work.

2.1.2. Thermal Boundary Conditions. Steady-state heat transfer is extensively used since it is simple to solve and verify the results with minimum tolerance [14]. The combustion process takes place in a short period of time, and it produces very high heat energy. The conductive mode of heat transfer will take more time, and the temperature change in the top layer of the piston is directly subjected to high heat zone [12, 15]. With the constant to-and-fro movement of the piston, there is change in heat transfer condition on the top of the piston, making the heat transfer state unstable. But logically, the piston will not absorb all of the heat produced by the combustion process; instead, the part of the heat energy will be transferred to the piston ring zone and cylinder liner, with some heat being evacuated via the exhaust. As a result, the temperature distribution on the piston is generally assumed to be in stable condition throughout analysis [16–18]. The

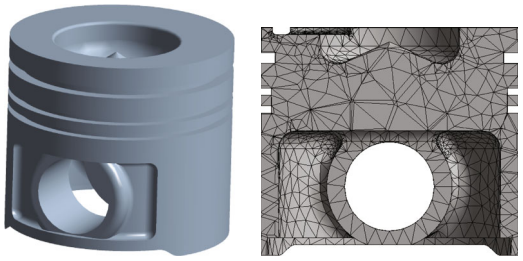

(a) Solid 3D model (b) Meshed model

Figure 4: Engine piston assembly model.

Table 2: Thermal boundary condition parameters for pistons with various alloying elements [10].

Position		Temperature (°C)	Film coefficient (W/m^2°C)
Piston crown	Outer	1140	489
	Central	1140	578
	Interior loop	1150	675
	Upper peripheral surface	1150	751
	Lower peripheral surface	1150	765
	Bottom	1150	486
Combustion chamber	Below the center	1150	395
	Above the center	1150	239
	Central top	1150	202
	Center	1150	328
Firepower shore		200	163
First ring groove	Upper surface	180	2260
	Bottom	180	2120
	Below surface	180	2223
First ring shore		180	470
Second ring groove	Upper surface	170	2080
	Bottom	170	1911
	Below surface	170	1972
Second ring shore		170	432
Third ring groove	Upper surface	150	1961
	Bottom	150	1909
	Below surface	150	2036
Third ring shore		150	325
Piston skirt		150	487
Oil return hole		150	778
Pin hole		140	324
Inner cavity	Upper surface	130	613
	Upper peripheral surface	100	435
	Middle peripheral surface	130	396
	Lower peripheral surface	130	335

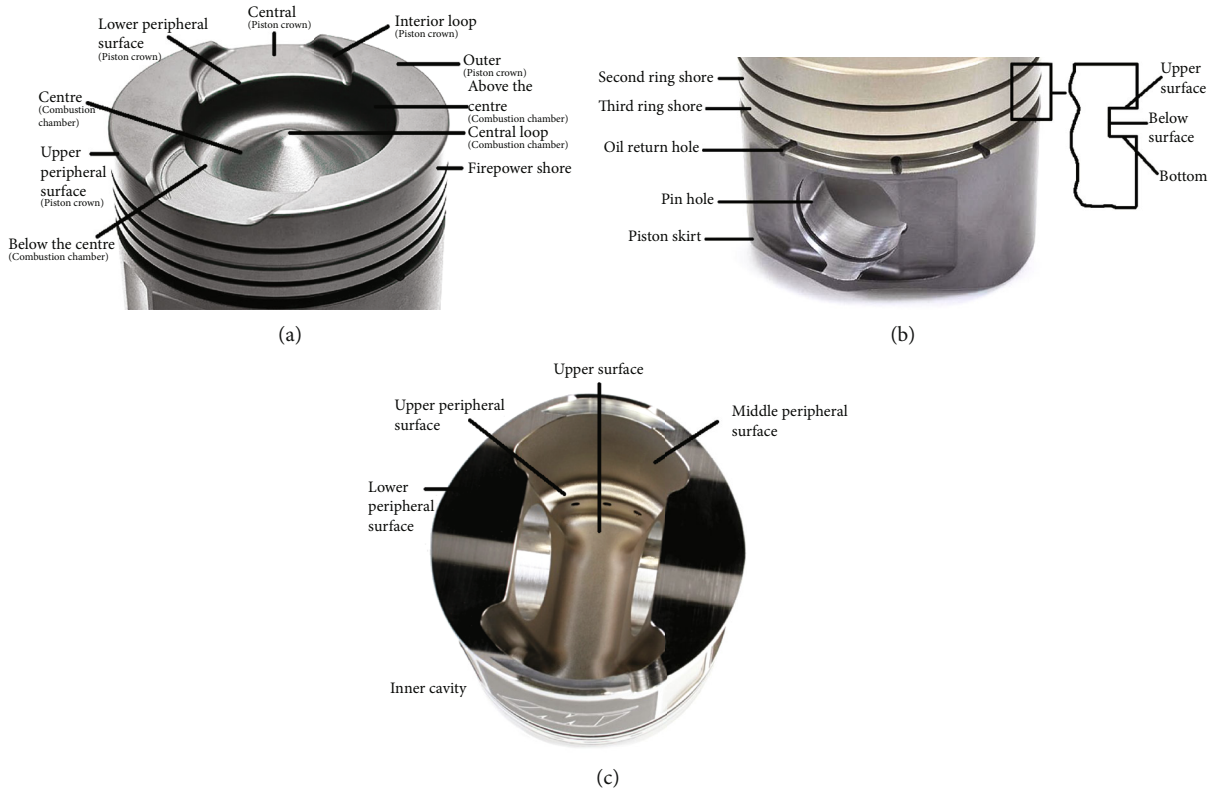

Figure 5: Positions mentioned as in Table 2.

Table 3: Material properties for piston materials, rings, and coating materials.

Material	Specific heat (J/kg°C)	Density (kg/m^3)	Thermal expansion 1×10^6 (1/°C)	Thermal conductivity (W/m^2°C)	Poisson's ratio	Young's modulus (GPa)
AlSi	910	2700	21	155	0.33	90
Steel	500	7870	12.2	79	0.3	200
NiCrAl	764	7870	12	16.1	0.27	90
MgZrO3	650	5600	8	0.8	0.2	46
Rings	460	7200	12	16	0.3	200

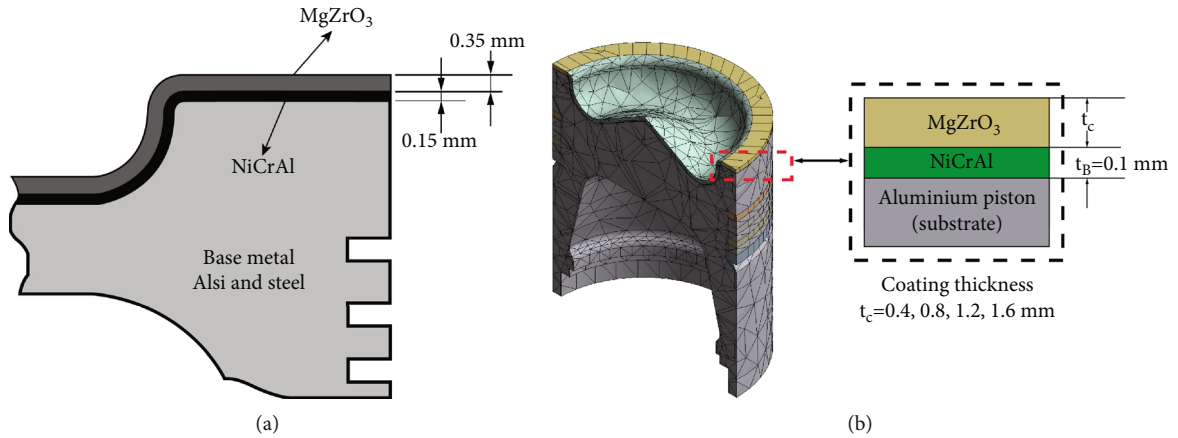

Figure 6: Thermal barrier coating thickness.

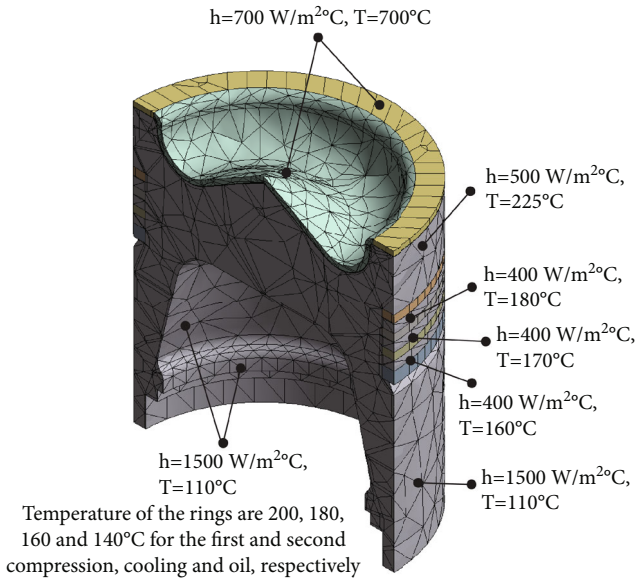

Figure 7: Thermal boundary conditions of piston.

major path of heat transmission, which includes the film coefficient and the tangential ambient temperature, is the third influencing parameter to consider for the piston surface temperature analysis. Thermal boundary conditions exist on the top surface layer of the piston, combustors, ring canal, ring shore, pin bore, piston skirt, and the inner cavity.

Table 2 manifests the thermal boundary conditions utilised in the finite element analysis which were obtained from the literature [10]. The location of the boundary conditions is mentioned in Figure 5 for more clarity to the readers.

2.2. Thermal Barrier Coating. Zirconia-based coatings are basically used in this study as the thermal barrier coatings. The unique and attractive thermal property of Zr material such as low thermal conductivity and high thermal expansion coefficient also helps in lowering the detrimental interfacial stresses. The material parameters of $MgZrO_3$, NiCrAl, and AlSi alloys, as well as steel piston materials, are listed in Table 3. For the illustration purpose, a 350 mm coating of $MgZrO_3$ is applied to the piston above a 150 mm layer of NiCrAl bond coat which is shown in Figure 6. The top layer of the thermal barrier coating employed with magnesia-stabilized zirconia ($MgZrO_3$). The unique behaviour of the material is having exceptional thermal insulating characteristics and stability in extreme temperature; it was chosen for this study [19–21] and has a compressive strength of 1450 MPa and flexural strength of 520 MPa [16]. The coating material is considered on the top of the AlSi alloy and steel piston, and the finite element analysis is carried out. The detailed description of the simulation conditions is discussed in the following section.

2.3. Finite Element Method Formulation. The piston model is imported to Ansys workbench as .stl file and rectified the errors associated with sharp edges and negligible wall thickness in the geometry. The model was discretized with an appropriate number of elements as in Figure 3. The model specifies the default bonded contact between the piston ring and the ring grove. The thermal parameters for piston are given as the ring land and skirt, the piston pin, the combustion side, and the underside thermal boundary condition. The ambient temperature and the film coefficient were calculated using published data [7, 21–24]. The temperature value for the first compression ring is 200 Â˚C, 180 Â˚C for second compression ring, 160 Â˚C for the cooling ring, and 140 Â˚C for the oil ring, respectively. In Figure 7, the average film coefficient and calculated temperatures are shown as boundary conditions.

3. Results and Discussion

3.1. Influence of Alloying Elements. The influence of the alloying element was taken in three combinations and compared in the bar chart for clarity on the influencing parameter. Figure 8 shows the outcomes of the thermal analysis for three different piston materials: A1, A2, and A3 that are listed in Table 1. The maximum temperature of the piston under thermal cycle conditions is expected to be 355 Â˚C at the neck of the combustor on the piston top. The temperature shows a noticeable temperature gradient and steadily decreases as other portions that are kept away from the fuel gas. Of all the components, the piston skirt has the lowest temperature since it is away from the top section. The surface temperatures of the three piston combustion chamber's neck, middle, and firepower shores were compared as in Figure 8. The outline of the results is shown in Figure 9 for more clarification with different factors. The temperature difference between A2 and A3 pistons is minimal due to the little variation in thermal conductivity of the material, but both values of temperature are higher than A1 piston, and also, the temperature difference of the piston combustor is bigger. The surface temperature of A3 piston is found to improve by 1.49% in compare to A1 piston and 0.73% in compare to A2 piston. In comparison to the A1 piston, the surface temperature of the A2 piston improves by 0.76%. As a result, when high-content alloying metals such as copper and nickel are introduced, it takes longer time for heat to move through the material as the material's thermal conductance is reduced and this will make a growth in the temperature of the piston surface and leads to less dissipation rate. Throughout the manuscript in all the contour plots, the field variable temperature (Â˚C) is considered with colour mapping motioned in the legend.

3.2. Influence of Ceramic Coating. The temperature for the standard and thermal barrier coated pistons was evaluated using numerical analysis. The results for the temperature distribution on AlSi alloy pistons with standard and ceramic coatings are shown in Figures 10 and 11. The highest temperature for a standard piston was determined to be 261 Â˚C. The rim of the piston bowl is where the temperature reaches its highest point since the surroundings are also in high temperature. The ceramic-coated piston reached a maximum temperature of 406 Â˚C. The piston bowl's top verge is where the temperature reaches its highest point. Because the largest temperature is transmitted to the serrated verge of the piston

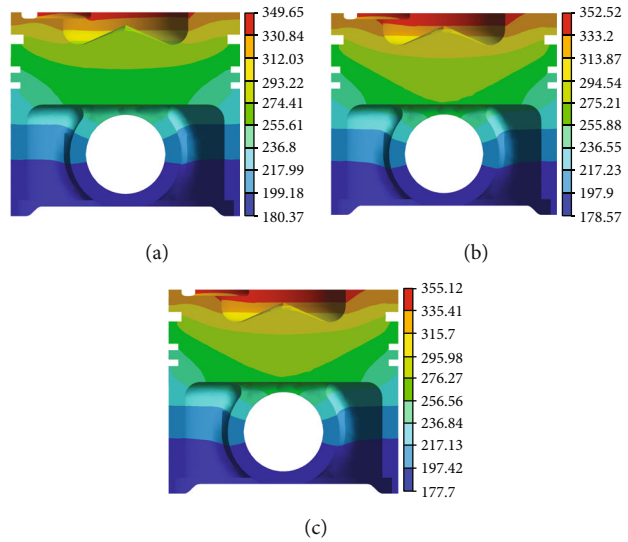

Figure 8: Temperature field distributions of piston with different alloying elements: (a) A1, (b) A2, and (c) A3.

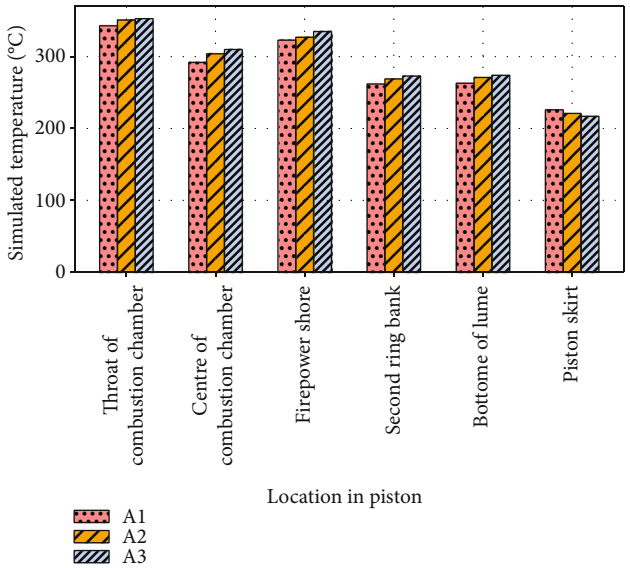

Figure 9: Results of a thermal analysis simulation of the surface temperature at various points on the piston.

from the piston rim, the rim has a larger convection area than the sharp edge. Heat transmission was greatly decreased because the lip surface was covered circumstantially with a ceramic substance which is having a low conduction coefficient.

It exhibits to raise the engine's combustor temperature slightly more. The base metal is not exposed to nearly as much thermal stress as the other metals. Additionally, it indicates that the requirements for the cooling of the system have decreased. The temperature circulation on standard and coated steel pistons is manifested in Figures 10 and 11. For the standard piston, the highest temperature in the combustion chamber is 316 Â°C. The maximum temperature of a coated steel piston on the edges of the combustion chamber was found to be 460 Â°C. The base metal of the coated piston reaches the highest temperature of 326 Â°C. The coated piston's lifetime is prolonged, and the cooling load is reduced as a result. The addition of a ceramic coating increases the surface temperature of an AlSi piston by about 55%. This enhanced value is roughly 45% for the steel piston compared to the alloying piston. Steel pistons reach temperatures close to 40 Â°C to 80 Â°C greater than aluminum pistons. The ceramic-coated steel piston outperforms the ceramic-coated AlSi alloy by approximately 13%.

3.3. Influence of Ceramic Coating with Different Thicknesses. The temperature distribution for uncoated pistons and pistons with variable coating thicknesses of the top coat is discussed in detail in this paper, which is based on the findings of thermal stress calculations using the finite element approach. Temperature distribution results for the piston without coating are shown in Figure 12. High temperatures may be detected at the center of the crown and the lip of the bowl of an uncoated piston. It was to be anticipated, given the piston's proximity to the heat flow. As shown in Figure 12, the highest temperature is located in the middle and on the piston top surface; the lowest temperature is observed towards the bottom of the crown bowl. The maximum temperature value is to be found 301.08 Â°C. Heat rises to the bowl lips, then dips back down again near the crown surface, in a circular pattern.

Counterplots of temperature distributions for ceramic coating thicknesses ranging from 0.04 cm to 0.16 cm are presented in Figure 13 under the same circumstances. The highest temperatures are 400.45 Â°C, 449.34 Â°C, 528.55 Â°C, and 550.5 Â°C, respectively, at the crown center of the piston on the surface of the coating. The maximal temperature was found on the crown center for coatings and is 24.63%, 32.83%, 42.9%, and 45.17% higher than the uncoated piston, respectively. Despite the fact that the thickness of the coating increases in a predictable way, the temperature does not. The maximum temperature rises as the coating thickness rises.

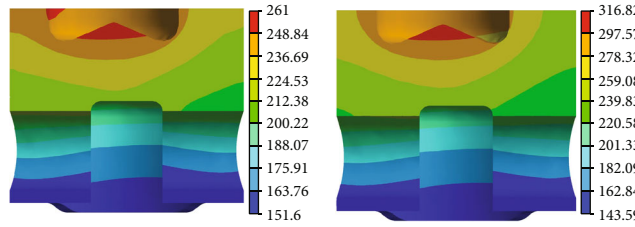

(a) AlSi alloy (b) Steel

Figure 10: Temperature distribution of a standard steel and an AlSi alloy piston.

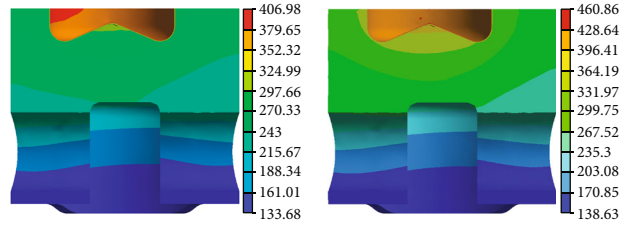

(a) AlSi alloy (b) Steel

Figure 11: Temperature distribution of ceramic-coated steel piston and ceramic-coated AlSi alloy piston.

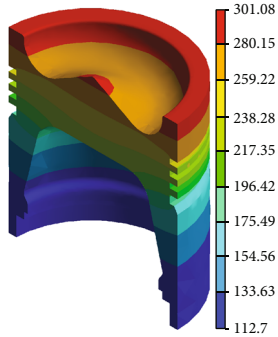

Figure 12: The temperature distribution of the uncoated piston.

Due to the ceramic's low heat conductivity in comparison to the aluminum alloy, the piston's head top surface reaches its maximum temperature with a 0.16 cm thick covering, as projected. Increment in temperature on the top of the piston's surface is proportional to the thickness of the covering. The strength of a material is known to be affected by temperature. As a result, it diminishes as the temperature rises. Lowering the working temperature improves the piston's strength, resulting in longer piston life.

3.4. Influence of Having Holes in the Ceramic Coating. The piston's center and bowl lips have the highest temperature, while the skirt of the piston has the minimal temperature. For an uncoated piston, the maximum and minimum temperatures are at 301.08 Â°C and 112.7 Â°C, respectively. The upper surface of the coated piston reaches a maximum temperature of 400.45 Â°C, 449.34 Â°C, 528.55 Â°C, and 550.5 Â°C for 0.04 cm, 0.08 cm, 0.12 cm, and 0.16 cm top coat thickness. The lowest temperature recorded was 114.63 Â°C, 113.06 Â°C, 112.35 Â°C, and 111.85 Â°C for 0.04 cm, 0.08 cm, 0.12 cm, and 0.16 cm top coat thickness. Thermal analysis on a piston with a magnesia-stabilized zirconia coating with holes for different coating thicknesses is performed using the same boundary conditions. Figure 14 depicts the temperature circulation on the coated piston's top surface with 1.5 mm radius holes. For 0.04 cm, 0.08 cm, 0.12 cm, and 0.16 cm coating thickness, the maximum top surface temperature for 1.5 mm radius holes is 440.86 Â°C, 500.79 Â°C, 575.9 Â°C, and 604.39 Â°C, which is 31.54%, 39.73%, 47.5%, and 50% higher than the temperature of the uncoated piston top surface. The temperature of the coated piston with no holes rises by 9.16%, 10.27%, 8.22%, and 8.92% for 0.04 cm, 0.08 cm, 0.12 cm, and 0.16 cm coating thicknesses, respectively, compared to the temperature of piston with coating and having no holes.

4. Conclusions

The steady-state thermal analysis was performed on the piston with the following variable parameters:

(i) Parametric study on alloying element

(ii) Different coating thicknesses

(iii) Coating with holes on the piston surface

The following points are concluded based on the results from the simulation. It is observed that

(1) A1 piston with higher contents of copper and nickel has lower temperature than A2 and A3, which shows that adding alloying elements to a material may alter its thermal conductance, affecting the temperature circulation of the piston exterior

(2) the value of surface temperature was increased about 55% for AlSi and 45% for steel piston and , the value

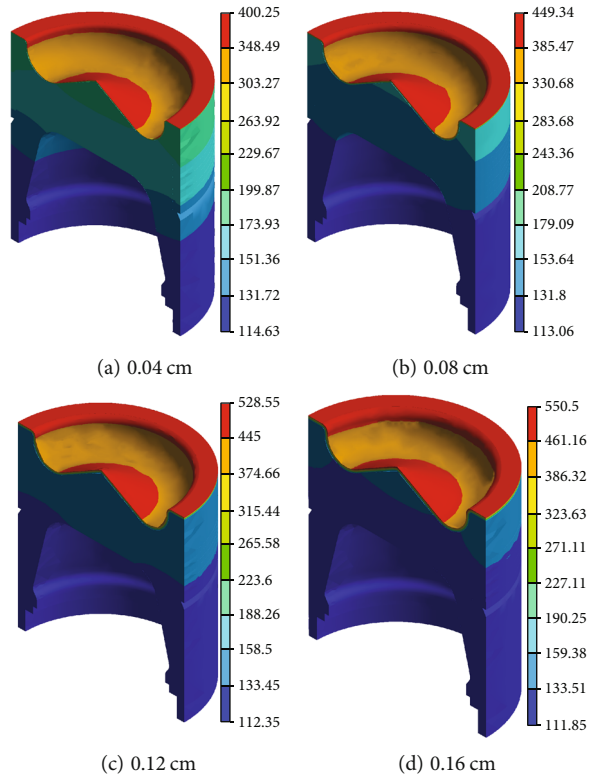

(a) 0.04 cm (b) 0.08 cm

(c) 0.12 cm (d) 0.16 cm

Figure 13: Top-surface temperature circulation for various coating thicknesses.

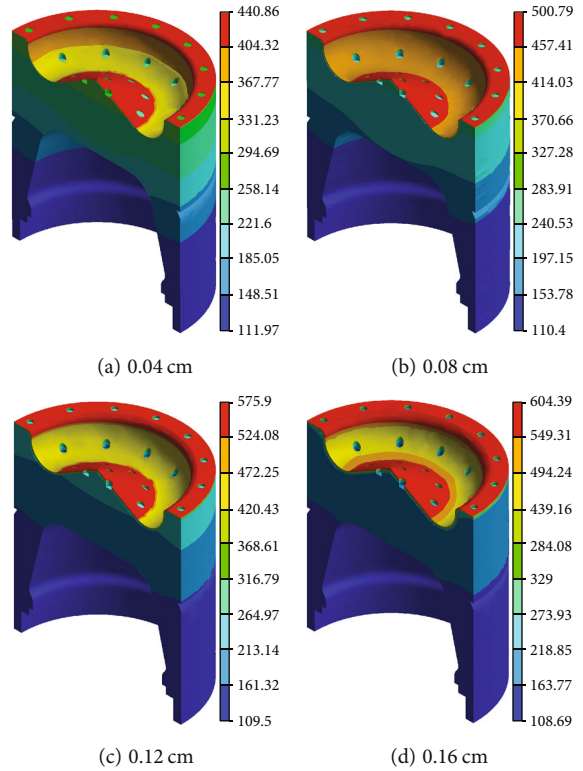

(a) 0.04 cm (b) 0.08 cm

(c) 0.12 cm (d) 0.16 cm

Figure 14: Temperature (Â°C) distribution of the top coating surface with holes of 1.5 mm radius for various coating thickness.

for steel piston is 11.7% higher than that of the AlSi piston. The highest value of temperature for the coated piston was found at the combustion bowl rim

(3) similarly, the values of maximum temperature at the piston surface for 0.04 cm-0.16 cm coating thickness are 24.63%, 32.83%, 42.9%, and 45.17% higher than the value of the standard piston without any coating

(4) In the same way, the highest temperature values for the piston having holes in the top coat are 9.16%, 10.27%, 8.22%, and 8.92% higher than those of the piston without holes and 31.54%, 39.73%, 47.5%, and % higher than the uncoated piston

From the observation, coating with hole has shown good agreement with better thermal efficiency for the piston application compared to the varying alloying elements and varying coating thicknesses. The varying coating materials and shapes of the holes in the coating surface and its influence on the thermal behaviour for the piston application with cooling channel are for future communication.

Data Availability

The dataset used in this paper is available from the corresponding author upon request.

Conflicts of Interest

The authors declare that they have no conflicts of interest.

Acknowledgments

This study was supported by Natural Science Foundation of Guangdong Province (2021A1515010467).

References

[1] A. Uzun, I.^. Çevik, and M. Akçil, "Effects of thermal barrier coating on a turbocharged diesel engine performance," *Surface and Coatings Technology*, vol. 116-119, pp. 505–507, 1999.

[2] T. Hejwowski and A. Wero'nski, "The effect of thermal barrier coatings on diesel engine performance," *Vacuum*, vol. 65, no. 3, pp. 427–432, 2002.

[3] A. Alkidas, *Performance and emissions achievements with an uncooled heavy-duty, single-cylinder diesel engine*, SAE International in United States, 1989.

[4] A. C. Alkidas, *Experiments with an uncooled single-cylinder open-chamber diesel*, SAE International in United States, 1987.

[5] V. Reghu, N. Mathew, P. Tilleti, V. Shankar, and P. Ramaswamy, "Thermal barrier coating development on automobile piston material (Al-Si alloy), numerical analysis and validation," *Materials Today: Proceedings*, vol. 22, pp. 1274–1284, 2020.

[6] M. Cerit, "Thermo mechanical analysis of a partially ceramic coated piston used in an SI engine," *Surface and Coatings Technology*, vol. 205, no. 11, pp. 3499–3505, 2011.

[7] H. Ng and Z. Gan, "A finite element analysis technique for predicting as-sprayed residual stresses generated by the plasma spray coating process," *Finite Elements in Analysis and Design*, vol. 41, no. 13, pp. 1235–1254, 2005.

[8] J. G. Muchai, A. D. Kelkar, D. E. Klett, and J. Sankar, "Thermal-mechanical effects of ceramic thermal barrier coatings on diesel engine piston," *MRS Online Proceedings Library*, vol. 697, article 810, 2002.

[9] A. Gilbert, K. Kokini, and S. Sankarasubramanian, "Thermal fracture of zirconia-mullite composite thermal barrier coatings under thermal shock: an experimental study," *Surface and Coatings Technology*, vol. 202, no. 10, pp. 2152–2161, 2008.

[10] T. Liu, A. Li, C. Zhu, and W. Yuan, "Effect of alloying elements on surface temperature field of aluminum piston in diesel engine," *Engineering Failure Analysis*, vol. 134, article 106020, 2022.

[11] R. Gehlot and B. Tripathi, "Thermal analysis of holes created on ceramic coating for diesel engine piston," *Engineering*, vol. 8, pp. 291–299, 2016.

[12] T. Uchimi, K. Taya, Y. Hagihara, S. Kimura, and Y. Enomoto, "Heat loss to combustion chamber wall in a D.I. diesel engine — First report: Tendency of heat loss to piston surface," *JSAE Review*, vol. 21, no. 1, pp. 133–135, 2000.

[13] P. S. Prakash Varma and K. Venkata Subbaiah, "A review on thermal and CFD analysis of 3 different piston bowl geometry's," *Materials Today: Proceedings*, vol. 37, pp. 2341–2345, 2021.

[14] S. Sharma and P. Dhakar, "A review study of steady state thermal analysis of piston by finite element method (FEM)," *International Journal of IC Engines and Gas Turbines*, vol. 4, no. 1, pp. 34–39, 2018.

[15] D. Robinson and R. Palaninathan, "Thermal analysis of piston casting using 3-D finite element method," *Finite Elements in Analysis and Design*, vol. 37, no. 2, pp. 85–95, 2001.

[16] M. Cerit and M. Coban, "Temperature and thermal stress analyses of a ceramic-coated aluminum alloy piston used in a diesel engine," *International Journal of Thermal Sciences*, vol. 77, pp. 11–18, 2014.

[17] H. Shete, R. Pasale, and E. Eitawade, "Photoelastic stress analysis & finite element analysis of an internal combustion engine piston," *International Journal of Scientific and Engineering Research*, vol. 3, no. 7, p. 1, 2012, https://www.ijser.org/viewPaperDetail.aspx?I015917.

[18] Y. Lu, X. Zhang, P. Xiang, and D. Dong, "Analysis of thermal temperature fields and thermal stress under steady temperature field of diesel engine piston," *Applied Thermal Engineering*, vol. 113, pp. 796–812, 2017.

[19] E. Buyukkaya and M. Cerit, "Thermal analysis of a ceramic coating diesel engine piston using 3-D finite element method," *Surface and Coatings Technology*, vol. 202, no. 2, pp. 398–402, 2007.

[20] T. M. Yonushonis, "Overview of thermal barrier coatings in diesel engines," *Journal of Thermal Spray Technology*, vol. 6, no. 1, pp. 50–56, 1997.

[21] E. Buyukkaya, "Thermal analysis of functionally graded coating AlSi alloy and steel pistons," *Surface and Coatings Technology*, vol. 202, no. 16, pp. 3856–3865, 2008.

[22] Z. Yao and W. Li, "Microstructure and thermal analysis of APS nano PYSZ coated aluminum alloy piston," *Journal of Alloys and Compounds*, vol. 812, article 152162, 2020.

[23] V. Esfahanian, A. Javaheri, and M. Ghaffarpour, "Thermal analysis of an SI engine piston using different combustion boundary condition treatments," *Applied Thermal Engineering*, vol. 26, no. 2-3, pp. 277–287, 2006.

[24] T. Sachit, R. Nandish, and Mallikarjun, "Thermal analysis of Cr_2O_3 coated diesel engine piston using FEA," *Materials Today: Proceedings*, vol. 5, no. 2, pp. 5074–5081, 2018.